

Developing a Predictive Product Failure Model for Polyurethane Treaded Wheels based on Loads and Speeds

Caster Concepts, Inc.

Written By: Mr. Douglas S. Backinger and Dr. Elmer Lee

Introduction

It is commonly understood that, for polyurethane treaded wheels, the prominent mode of failure is that of the bond between the tread and hub. While numerous factors can create such a failure mode, the predominant mechanism leading to bond failure is excessive heat in the bond region. Such heat is typically generated by the tread itself. Subjected to continuous deformation, the urethane tread transforms this mechanical deformation, through the hysteresis of the material, into thermal energy. As the temperature rises, the bond degrades ultimately leading to failure.

Polyurethane tires can build up heat from high speeds, high loads or a combination of both. The large impact of load and speed on a wheel makes it very important to know the operating conditions in order to avoid tire failure.

We were requested by Caster Concepts, Inc. (CCI) to develop a procedure that would predict failure in their polyurethane-treaded wheels based on both the load and speed of the wheel. A predictive failure formula would be very useful to CCI. The formula would provide a better understanding of the polyurethane tires and how they will react to various combinations of load and speed. It would allow consumers to purchase the right tread and wheel combination, designed precisely to meet their application needs.

The purpose of this paper is to describe the process developed to create a predictive wheel failure model and elaborate on the results and conclusions from the tests performed to obtain a predictive failure equation. The first section of the paper will state our procedure and the theory behind the experiments. The second section will give the results from our experiments and the final section will state the conclusions.

Summary of Results

Polyurethane tires generate heat from the hysteresis of the urethane when it is cyclically deformed under load. This energy generation can be related to the load and speed of the wheel. The energy is absorbed by the wheel core or expelled through convective heat loss. The fluid velocity of air is caused by the rotation of the wheel. When the energy absorbed and the energy lost to convection are summed together, they equal the energy generated by the cyclic deformation. An equation can be derived from the conservation of energy equation of the complete system that can predict the final temperature the wheel will reach. Based off of temperature failure data and the final predicted temperature, the failure of a wheel can be predicted given a specified load and speed.

Predictive failure equation: The predictive failure equation is:

$$\frac{1}{2hA} \left(k_{HG} \frac{v}{R^{\frac{5}{3}}} L^{\frac{4}{3}} \left(\frac{S}{W} \right)^{\frac{4}{3}} \right) + T_{AMB} = T_{\infty} (\text{°C}) \pm 5\% \quad (1)$$

Theory

To determine the steady state temperature of (and hence failure of) a polyurethane-treaded wheel at a given load and speed, the total energy into and out of the system must be examined. The rudimentary conservation of energy equation is as follows:

$$E_{gen} = E_{absorbed} + E_{out} \text{ (J)} \quad (2)$$

The source of the energy into the system (E_{gen}) is from the deformation of the polyurethane tire. The energy absorbed ($E_{absorbed}$) by the system is the rise in its temperature (or change in internal energy), and the energy out of the system (E_{out}) is the energy removed from the system through convective heat transfer. The energy generation can be modeled by equation (3).

$$E_{gen} = k_{HG} \frac{v}{R^3} t L^3 \left(\frac{s}{w}\right)^3 \text{ (J)} \quad (3)$$

In (3), E_{gen} is the energy generated in (J), k_{HG} is a material constant which describes heat generation, v is the tangential velocity in m/s, R is the wheel radius in meters, t is time in seconds, L is the load in newtons, s is the tire thickness in meters, and w is the tire width in meters. The energy generation equation was developed from the knowledge that urethane generates heat when it is deformed. The heat generation is due to the internal friction of the urethane polymer chains sliding past each other during deformation. The amount of deformation can be calculated using the widely accepted formula for urethane tire deflection shown in (4). The energy generated through the deflection of the tire can be approximated with the potential energy equation for springs, shown in (5). Equation (5) assumes a linear spring model and that a percentage of the spring deformation energy is transformed into thermal energy. The rate of the heat generation is governed by the inherent chemical nature of the urethane and the frequency at which the deformation occurs.

$$U = \left(\frac{0.75 L s}{E w (8R)^2} \right)^{\frac{2}{3}} \text{ (m)} \quad [1] \quad (4)$$

Where U is the tire deflection in meters, L is the load in newtons, s is the thickness of the urethane tire in meters, E is the compressive modulus of the urethane in Pascals, w is the width of the tire in meters, and R is the radius of the wheel in meters.

$$E_{gen} = k_{HG} E_{Spring} = \frac{1}{2} k_{HG} k_{spring} U^2 \quad (5)$$

Where E_{Spring} is the potential energy of a spring in Joules, k_{spring} is the spring constant in Joules per meter squared, and U is the deflection of the spring in meters. Equation (3) is formed when (4) is plugged into (5). The 0.75 and compressive modulus (E) are constants, so they are taken from (4) and lumped in with the heat generation coefficient, k_{HG} in (3).

The energy absorbed by the wheel is modeled by (6), which is a heat transfer formula for change in internal energy for a lumped capacitance model.

$$E_{ABS} = MC_p \Delta T \text{ (J) [2]} \quad (6)$$

Where E_{ABS} is the energy absorbed by the wheel, M is the mass of the wheel (kg), C_p is the specific heat of the wheel (J/kg-°C), and ΔT (°C) is the temperature difference between the current temperature of the wheel and the initial temperature of the wheel.

The energy leaving the wheel is modeled as surface convection, with radiation and conduction effects being neglected. Conduction can be neglected by showing that the Biot number is less than 0.1. When the Biot number is small, the temperature gradient in a body goes to zero. The body can then be treated as a uniform temperature, i.e. a lumped capacitance model. The Biot number is defined as the ratio of the conduction resistance to the convection resistance. Radiation can be neglected if the temperatures of the objects are relatively low. The temperatures seen in this experiment are low (<100°C), so radiation effects can be neglected. Convective heat transfer will dominate over the other modes because the wheel is spinning, which generates a fluid air velocity. The convective heat transfer equation is shown below:

$$E_{Out} = 2hAt \Delta T_{Out} \text{ (J) [3]} \quad (7)$$

Where E_{Out} is the convective heat transfer energy, h is the convective heat transfer coefficient (W/°C-m²), A is the surface area of one side of the wheel (m²), t is the time (s), and ΔT_{Out} is the temperature difference between the wheel (T_W) and the ambient temperatures (T_{AMB}) in °C. The equation must be multiplied by two because there are two faces of the wheel that are experiencing the convective heat loss.

When the energy flux by the wheel and the heat flux due to convection are summed together, they will equal the heat flux generated by the deformation of the polyurethane. This equation is shown below:

$$\frac{d}{dt} \left(k_{HG} \frac{v}{R^3} L^3 \left(\frac{s}{W} \right)^{\frac{4}{3}} \right) = 2hAt \Delta T_{Out} + MC_p \Delta T \text{ (W)} \quad (8)$$

This equation simplifies into a linear first-order ordinary differential equation:

$$k_{HG} \frac{v}{R^3} L^3 \left(\frac{s}{W} \right)^{\frac{4}{3}} = MC_p \frac{dT_W}{dt} + 2hA(T_W - T_{AMB}) \quad (9)$$

In Equation 9, the unknowns variables are k_{HG} and hA , to be determined through experimentation. Equation (9) is solved using initial and final condition variables, T_i (at time equal to 0) and T_∞ (at time equal to infinity), to yield the following equation for the temperature profile of the wheel:

$$T_W(t) = (T_i - T_\infty) e^{\frac{-2hAt}{MC_p}} + T_\infty \quad (10)$$

Where $T_w(t)$ is the temperature of the wheel at a given time, t is the time in seconds, T_i is the initial temperature of the wheel and T_∞ is the steady state temperature of the wheel in °C. From (9) and (10), two more equations, (11) and (12) respectively, can be derived to solve the two unknowns, k_{HG} and hA .

$$k_{HG} = \frac{2hA(T_\infty - T_{AMB})}{\frac{v}{R^3} L^3 \left(\frac{s}{w}\right)^3} \quad (\text{J}\cdot\text{m}^{2/3}/\text{N}^{4/3}) \quad (11)$$

$$hA = -\frac{MC_p}{2t} \ln\left(\frac{T_w(t) - T_\infty}{T_i - T_\infty}\right) \quad (\text{W}/^\circ\text{C}) \quad (12)$$

When (10) is evaluated as time goes to infinity, the transient terms go to zero. This leaves an equation that can be arranged to solve for the final temperature of the wheel. The equation is:

$$\frac{1}{2hA} \left(k_{HG} \frac{v}{R^3} L^3 \left(\frac{s}{w}\right)^3\right) + T_{AMB} = T_\infty \quad (^\circ\text{C}) \quad (13)$$

This equation can be used to predict the final temperature of the wheel, and thus the speed and load at which the tire will fail. With the analysis complete, tests can be run to obtain the data necessary to evaluate the equations, specifically for k_{HG} and hA .

Procedure

Testing was conducted in the Engineering Testing Laboratory at CCI. All tests were run in a temperature controlled environment, with an ambient temperature of $22^\circ \pm 3^\circ \text{C}$ and at 1 atm. The Dynamic Wheel Endurance Test Machine (DWET) was used to conduct all tests. A picture of the test machine can be seen in Figure 1.

The tests were run with various size wheels from the CCI product line. The testing included wheels of size diameter 0.15, 0.20, and 0.25 meters (6, 8 and 10 inches respectively) and widths of 0.05 and 0.08 m (2 and 3 inches respectively).

All wheels had a thin tread (3/8 inches or 0.010 m) of CCI's 85 A polyester MDI polyurethane and a cast iron core. This urethane has a failure temperature of $60 \pm 5^\circ\text{C}$, determined through previous testing. The wheels were held in a rigid caster and all were equipped with (2) precision ball bearings. The values for MC_p for all wheel



Figure 1: Wheel Endurance Test Machine at CCI

sizes are listed in Appendix A.1. The value for C_p of cast iron is 460 J/kg-°C Table 1 shows the number of tests run on each size wheel. The total number of tests run was 30. Each size group was run under various load and speed parameters. The loads varied from 1,600 N to 8,100 N and the speeds varied from 0.9 m/s to 2.8 m/s. The parameters and results can be seen in Appendix A.1.

Table 1: Predictive Failure Model Test Set

Wheel Size (m)	# of Tests
0.20 x 0.05 (8x2 in)	9
0.20 x 0.08 (8x3 in)	6
0.15 x 0.05 (6x2 in)	4
0.15 x 0.08 (6x3 in)	6
0.25 x 0.08 (10x3 in)	5

A custom program was written using National Instruments LabView software to set the load and speed the wheels will be tested at. The wheels were then loaded into the test machine and clamped down. An IR sensor, Raytek model RAYCI3A10L, was placed on the test machine to measure the inside web temperature of each wheel. A picture of the setup is shown in Figure 2. The specified load was then applied to the wheel using a pneumatic bellows piston. Wheels were then tested using various test parameters (see Appendix A.1).



Figure 2: Setup of Experiment

The temperature, load, and speed data were all recorded by the LabView program. The test results are located in Appendix A.1. The data provided from these tests provided the information necessary to determine the unknown variables in the predictive failure equation. Figure 3 lays out the testing and data recording process that was used to develop the predictive failure model.

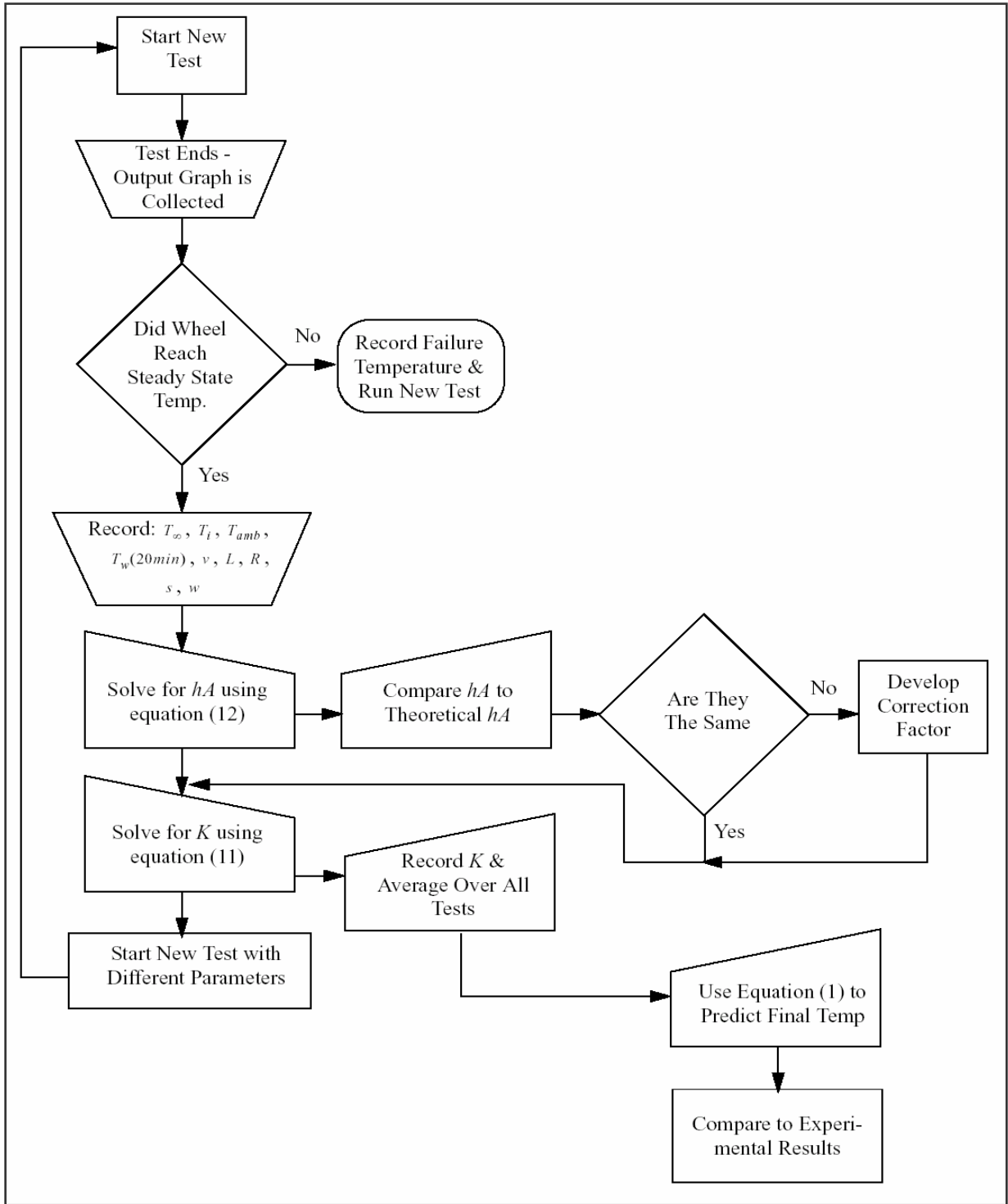


Figure 3: Flow chart showing testing process

Results

The test data was used to solve for the unknowns and to validate the predictive failure equation. The results are as follows:

Validation of lumped capacitance model: The Biot number formula is shown below:

$$Bi = \frac{R_k}{R_{ku}} \quad [3] \quad (14)$$

$$R_k = \frac{\ln(R_2 / R_1)}{2\pi L k_{thermal}} \quad [3] \quad (15)$$

$$R_{ku} = \frac{1}{hA} \quad [3] \quad (16)$$

R_k is the conduction resistance of the cast iron in °C/W, R_{ku} is the convection resistance in °C/W, R_2 is the outer radius of the cast iron core in m, R_1 is the inner radius of the cast iron core in m, L is the thickness of the wheel in m, $k_{thermal}$ is the thermal conductivity of cast iron in W/m-K, and hA is the convective heat transfer coefficient in W/°C. The conduction resistance is solved for in (15) and the convection resistance is found from (16).

The calculated Biot number is 0.10 ± 0.01 . Since it is equal to 0.10, the lumped capacitance assumption is still valid and the initial assumption can be assumed correct. The cast iron wheel can now be assumed to be at one uniform temperature throughout and conduction heat loss can be neglected. The calculation of the Biot number is shown in Appendix A.2.

Determination of unknown hA : The convective heat transfer coefficient h will vary as the speed of the wheel changes, while the surface area of the face of the wheel, A , remains constant. The value of h changes as the wheel speed varies because the faster the wheel spins the faster the ambient air is circulated around the wheel, causing heat to be removed at a faster rate. Since hA will vary, a theoretical equation was derived to estimate the value of the term at a given wheel speed. The equation for hA is shown in (17).

$$hA = \pi k_f R \left(0.3 \left(\frac{2}{3} \sqrt{\frac{vR}{\nu_f}} \right) \right) \quad (W/°C) \quad (17)$$

Where k_f is the thermal conductivity of air, R is the radius of the wheel in meters, v is the velocity of the wheel in m/s, and ν_f is the kinematic viscosity of air in m^2/s . The quantity $\frac{vR}{\nu_f}$ is the Reynolds number for a fluid moving over a spinning disc [3]. The equation for hA will only be valid for laminar air flows. These are air flows with a Reynolds number less than 240,000 [3]. The largest Reynolds number from our experiment was 12,571, so the equation for hA is valid in our calculations. The equation for hA was derived from Principles of Heat Transfer from the general equation for the convective h and the Reynolds Number for a rotating disc.

The value for hA was also solved for experimentally using (12). The theoretical values of hA for each wheel size at various speeds were compared to the experimental values. All theoretical

values of hA were below the experimental hA by an amount of $0.54 \pm 0.05 \text{ W/}^\circ\text{C}$. To compensate for the gap between the theoretical formula and experimental values, 0.54 was added to the formula for hA to give (18).

$$hA = \pi k_f R \left(0.3 \left(\frac{2}{3} \sqrt{\frac{vR}{\nu_f}} \right) \right) + 0.54 \pm 0.08 \text{ (W/}^\circ\text{C)} \quad (18)$$

Figure 4 shows the trend of experimental and theoretical hA values and also the corrected hA values for 8x2 wheels. The slopes of the experimental and theoretical hA values are very close in scale and the curves are almost equal once the 0.54 correction is added to the theoretical hA .

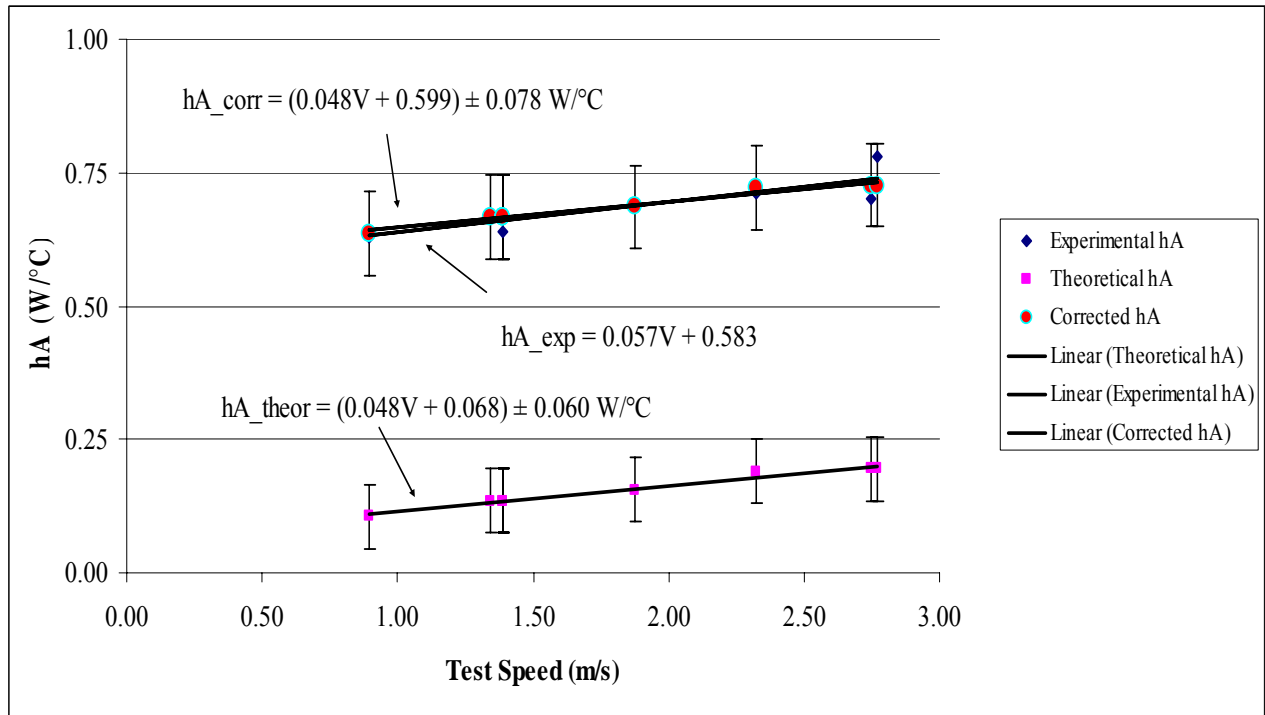


Figure 4: The corrected hA values coincide well with the experimental values

This additional $0.54 \pm 0.05 \text{ W/}^\circ\text{C}$ is believed to be due from the natural convection heat losses the wheel is experiencing. The natural convection heat loss is still influential at the low revolutions per minute (RPM) the wheels were tested at (less than 250 RPM) [4]. To test this theory, a cooling test was conducted in which an 8x2 wheel was run for 3 hours and allowed to reach a steady state temperature of 42°C . The wheel was then allowed to cool for 3 hours. It reached a final cooled temperature of 23°C . Its temperature after 20 minutes of cooling (33°C), after 0 minutes of cooling (initial hot of 42°C), and after reaching steady state (cooled at 23°C) were plugged into (10) to evaluate the hA of natural convection. The natural convection hA was measured to be approximately $0.42 \text{ W/}^\circ\text{C}$. This value agrees well with the $0.54 \text{ W/}^\circ\text{C}$ correction factor added into (18), showing that, indeed, natural convection plays a large part in the heat transfer model at low RPMs.

The natural convection heat loss is expected to change with surface area and substrate-ambient temperature differential. A constant natural convection heat loss is a close approximation for this model. This is because the temperature differentials between the hot wheel and ambient air are relatively small. The largest differential we expect when a wheel is running at a steady state temperature is 40°C. Most tests were run with an average temperature differential of 20°C.

The difference in surface area of the wheels as diameters vary will also affect the natural convection heat loss. A 10x3 (0.25x0.08 m) wheel will lose more heat to natural convection than a 6x2 (0.15 x 0.05 m) wheel. Since the hA add-in factor was calculated for the average wheel diameter of the tested wheels, which was 8 inches (0.20 m), the add-in factor became an average over the test set. The constant used will overestimate heat loss for 6 inch (0.15 m) wheels and underestimate natural convection heat loss for 10 inch (0.25 m) diameter wheels. However, we have shown that the resulting error is minimal. Finding a new constant for each wheel diameter is not necessary to achieve an acceptable level of accuracy of the hA formula (18) for all diameters of wheels.

Determination of the heat generation coefficient, k_{HG} : k_{HG} is the material constant in the heat generation equation (3). It is a material property, primarily dependant on the tread material used. It is not purely a material property because it is affected by the bond strength between the urethane tire and wheel core. If the bond is poor, the urethane will break free and slide against the wheel core. This friction adds more heat to the system, causing the urethane to fail prematurely.

Using the data from the tests, k_{HG} is solved using (11). The value of k_{HG} was found to be $5.5 \times 10^{-5} \pm 1.5 \times 10^{-5} \text{ J-m}^{2/3}/\text{N}^{4/3}$.

The constant k_{HG} will vary with each type of urethane tire. The higher the value of k_{HG} , the more heat the urethane will generate when deformed. All tests were done with CCI's 85 A MDI urethane, so the stated value of k_{HG} is only valid for that urethane.

Verification of Predictive Failure equation: The predictive failure equation is shown in (1). The equation was verified through extensive testing of various sizes of 85 A MDI treaded wheels.

$$\frac{1}{2hA} \left(k_{HG} \frac{v}{R^3} L^3 \left(\frac{S}{W} \right)^3 \right) + T_{AMB} = T_{\infty} (\text{°C}) \pm 5\% \quad (1)$$

The equation is accurate in predicting the final temperature of the wheel within $\pm 5\%$. The correct hA value based off of the speed the wheel will be traveling at can be estimated in (18). The values for v, L, and T_{AMB} are all chosen to meet the specific application. The value of k_{HG} will depend on the type of urethane being used. The k_{HG} values for various urethanes must be obtained experimentally.

The following graphs display the effectiveness of the formula in (1) in tracking the temperature profile of the test wheels. Equation (1) was used to predict the steady state temperature of the wheel and was then plugged into (10) to obtain the temperature profile of the wheel.

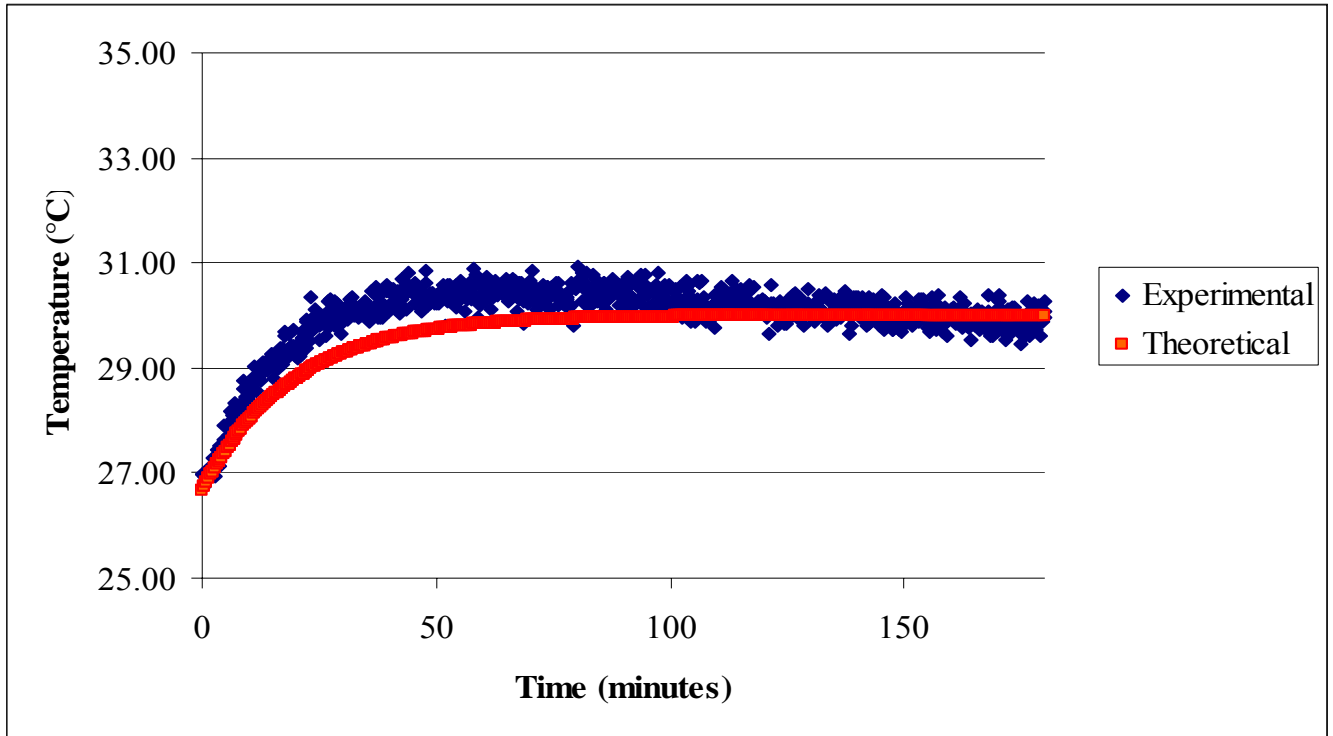


Figure 5: Actual vs. theoretical temperature profile of an 8x2 85 A Polyester MDI treaded wheel running at 0.9 m/s and 2,225 N (2 mph and 500 lbs).

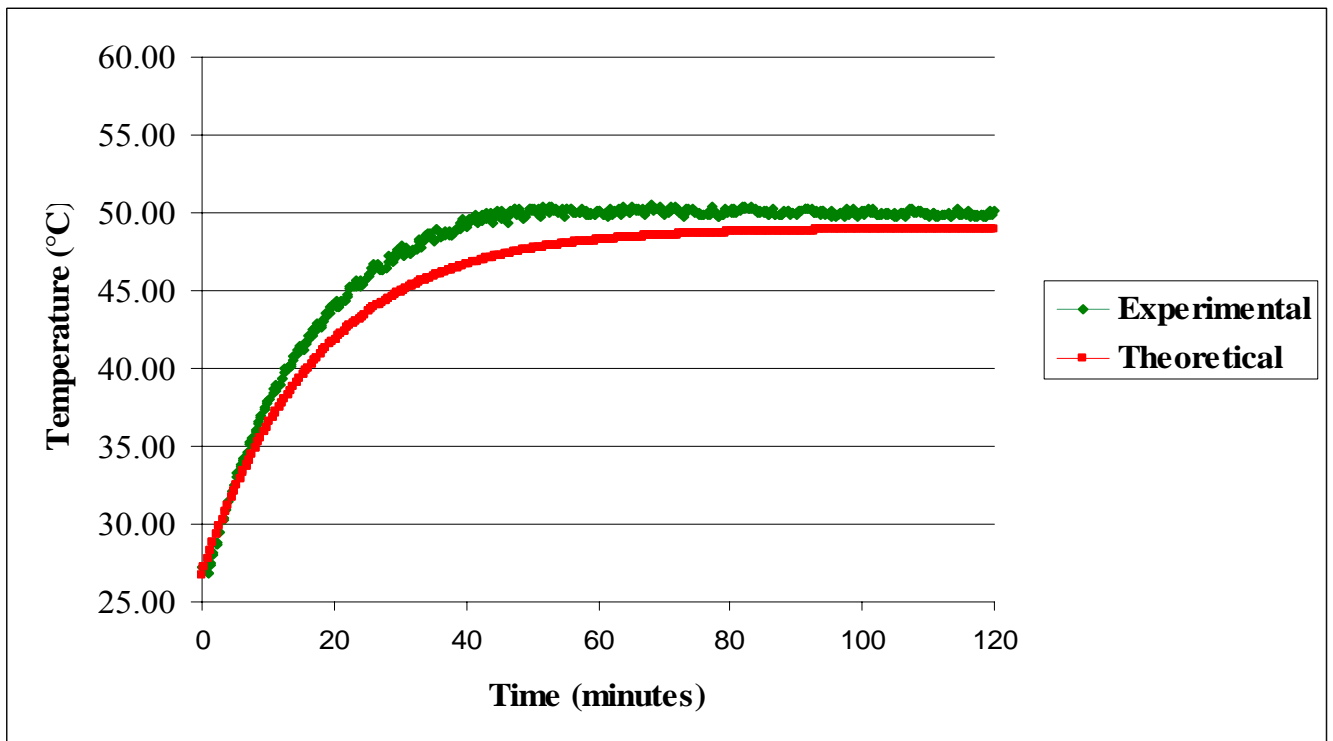


Figure 6: Actual vs. theoretical temperature profile of an 8x2 85 A Polyester MDI treaded wheel running at 2.24 m/s and 3,560 N (5 mph and 800 lbs).

The prediction equation does begin to break down when the tire deflection under load exceeds 10%. We believe that the linear spring model of the E_{gen} equation breaks down. Once 10% deflection is reached the heat generation begins to change and grows exponentially, so the wheels become more likely to fail. The deflection is calculated from a widely used and accepted formula for deflection in a urethane tread. The deflection formula and explanation is located in Appendix B.1.

The variations in the failure prediction equation, between theoretical and actual results, can be attributed to many different factors. Precision error in all of the computer sensors and equipment is listed at .05%. Force load cell resolution is approximately 111 N (25 pounds). The positioning of the IR sensor could also give a fluctuation in temperature readings of about $\pm 2^\circ\text{C}$. There is also some contributable human error in reading the temperature profile graphs, approximated at $\pm 1^\circ\text{C}$.

Conclusions

With (1), the final temperature of the wheel can be predicted from a given speed and load. This temperature can be compared to the failure temperature of $60 \pm 5^\circ\text{C}$ to determine if the polyurethane tire will withstand the applied load and speed. The equation will predict the final temperature within 5%. This equation can also be applied to wheels of different diameters and widths, with only a new hA value needing to be calculated. Figure 7 gives the predicted load/speed combinations that will result in failure for the specified wheel size. If the load/speed combination falls to the right of the curve for a specific wheel size, then the tire is predicted to fail. If the combination falls to the left of the curve, the wheel/tire combination will perform successfully at those parameters.

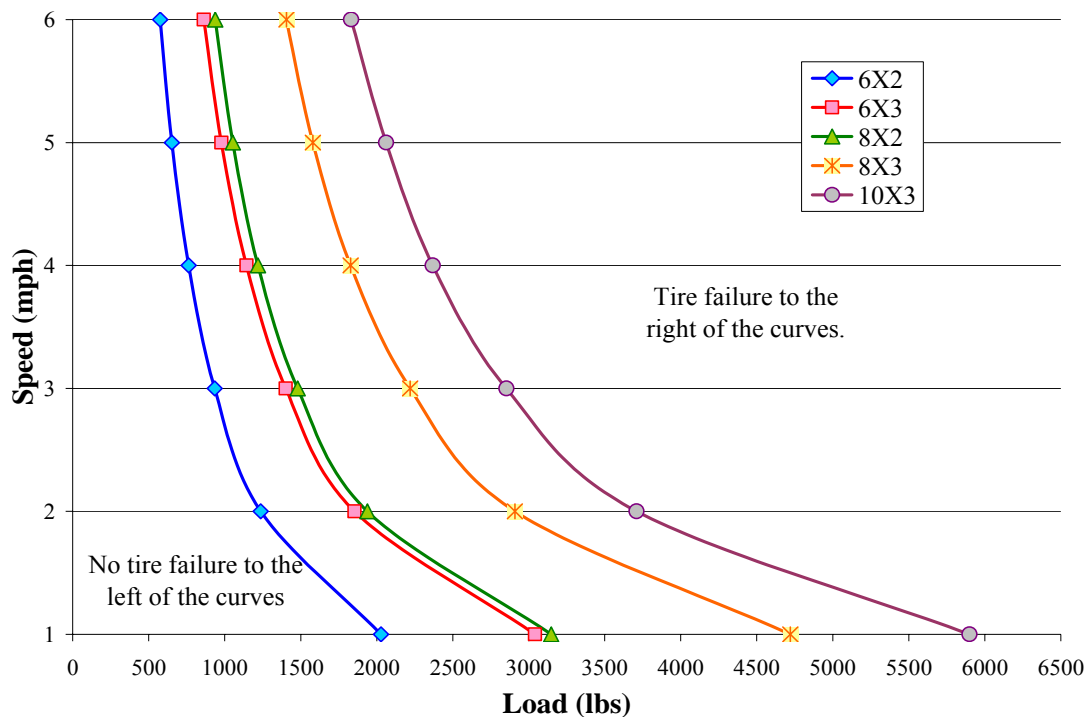


Figure 7: Combinations of Load and Speed to Induce Failure in CCI 85 A Polyurethane treaded wheels

The equation is only valid for thin-tread polyurethane tires. When the tread becomes thick (greater than 0.02 m (¾ inches)) the heat becomes trapped in the urethane due to its insulating properties, and the wheel does not follow the lumped capacitive model. Future studies will include a new model for thicker tread urethane tires.

The equation also begins to break down when tire deflection is greater than 10% of the thickness. This is due to the tire being overstressed which leads to the breakdown of the material as well as the heat generation. This greatly increases the speed of the failure process.

The heat generation coefficient derived in this test for the failure equation is only valid for Caster Concept's standard 85A polyurethane. To predict the failure of other types of polyurethane treads, new k_{HG} constants would have to be experimentally determined. This is because different types of urethanes generate different amounts of heat when deformed. The failure temperature is also only valid for the 85 A polyester MDI urethane. Further testing will be conducted to obtain k_{HG} values and failure temperatures for all types of urethane that CCI uses in their products.

The predictive failure model will be very useful for determining the correct wheel and urethane tire combination for specific applications without the need for testing. With the formula developed, only a few baseline tests are needed to develop the k_{HG} for any urethane. Once a baseline k_{HG} is developed, the formula can be used as a quality control tool to monitor tire/bond performance. Since k_{HG} is affected by the bond strength, a poor bond will yield a higher k_{HG} which can then be compared to the baseline. Variations in the urethane stoichiometry will also affect the k_{HG} and the performance of a wheel.

As testing continues at Caster Concepts, Inc. the database of urethane properties will continue to grow and become more refined. This will lead to a better understanding of the use of polyurethane in industrial tire applications.

References

- [1] Hoodbhoy, A I. "Designing with Plastics - Cast Solid-Polyurethane Industrial Tires." Plastics Engineering (1976): 37-38.
- [2] Rolle, Kurt C. Thermodynamics and Heat Power. 5th ed. Upper Saddle River, New Jersey: Prentice Hall, Inc., 1999. 20.
- [3] Kaviany, Massoud. Principles of Heat Transfer. New York: John Wiley & Sons Inc, 2002. 624.
- [4] Cardone, G., T. Astarita, and G. M. Carlomagno. "Infrared Heat Transfer Measurements on a Rotating Disk." Optical Diagnostics in Engineering 1 (1996): 1-7. 10 Sept. 2006.

Appendix A.1: Test Data

Test 1 8 x 2 85A				Test 2 8 x 2 85A			
Tw(t)	82.50	Tw(t) (C)	28.06	Tw(t)	93.00	Tw(t) (C)	33.89
Ti	73.00	Ti (C)	22.78	Ti	74.00	Ti (C)	23.33
Tinf	91.00	Tinf (C)	32.78	Tinf	104.00	Tinf (C)	40.00
Tamb	72.00	Tamb (C)	22.22	Tamb	74.00	Tamb (C)	23.33
V	3.10	V (m/s)	1.39	V	4.20	V (m/s)	1.88
L	500.00	L (N)	2224.91	L	660.00	L (N)	2936.88
t (s)	900.00	THICK	0.009525	t (s)	1200.00	THICK	0.009525
		WIDTH	0.0508			WIDTH	0.0508
k	0.000058			k	0.000047		
hA	0.64	-6.747078	0.9367938	hA	0.64	-10.03947186	0.9087648
hA_theory	0.68			hA_theory	0.70		
k av	0.0000545			k av	0.0000545		
Tinf pred	31	deg C		Tinf pred	41	deg C	
	89	deg F			105	deg F	
% diff	4.08			% diff	2.06		
diff	1.338502799	°C		diff	0.8236473	°C	

Test 3 8 x 2 85A				Test 4 8 x 2 85A			
Tw(t)	94.30	Tw(t) (C)	34.61	Tw(t)	100.00	Tw(t) (C)	37.78
Ti	78.00	Ti (C)	25.56	Ti	78.00	Ti (C)	25.56
Tinf	103.00	Tinf (C)	39.44	Tinf	111.00	Tinf (C)	43.89
Tamb	72.00	Tamb (C)	22.22	Tamb	72.00	Tamb (C)	22.22
V	3.00	V (m/s)	1.34	V	6.15	V (m/s)	2.75
L	800.00	L (N)	3559.85	L	675.00	L (N)	3003.63
t (s)	1200.00	THICK	0.009525	t (s)	1200.00	THICK	0.009525
		WIDTH	0.0508			WIDTH	0.0508
k	0.000056			k	0.000045		
hA	0.67	-0.83091	0.9917594	hA	0.70	-5.396170296	0.9488011
hA_theory	0.68			hA_theory	0.74		
k av	0.0000545			k av	0.0000545		
Tinf pred	39	deg C		Tinf pred	47	deg C	
	102	deg F			117	deg F	
% diff	1.20			% diff	7.96		
diff	0.473916517	°C		diff	3.4954682	°C	

Test 5 8 x 2 85A				Test 6 8 x 2 85A			
Tw(t)	92.00	Tw(t) (C)	33.33	Tw(t)	95.00	Tw(t) (C)	35.00
Ti	75.00	Ti (C)	23.89	Ti	80.00	Ti (C)	26.67
Tinf	101.00	Tinf (C)	38.33	Tinf	101.00	Tinf (C)	38.33
Tamb	71.00	Tamb (C)	21.67	Tamb	72.00	Tamb (C)	22.22
V	3.10	V (m/s)	1.39	V	6.20	V (m/s)	2.77
L	800.00	L (N)	3559.85	L	500.00	L (N)	2224.91
t (s)	1200.00	THICK	0.009525	t (s)	1200.00	THICK	0.009525
		WIDTH	0.0508			WIDTH	0.0508
k	0.000052			k	0.000056		
hA	0.68	-0.663017	0.9934135	hA	0.80	7.472198225	1.0807562
hA_theory	0.68			hA_theory	0.74		
k av	0.0000545			k av	0.0000545		
Tinf pred	39	deg C		Tinf pred	39	deg C	
	102	deg F			103	deg F	
% diff	1.52			% diff	2.27		
diff	0.581861815	°C		diff	0.8718663	°C	

8x3 85A		Test 1	
Tw(t)	87.00	Tw(t) (C)	30.56
Ti	77.00	Ti (C)	25.00
Tinf	98.00	Tinf (C)	36.67
Tamb	74.00	Tamb (C)	23.33
V	3.00	V (m/s)	1.34
L	820.00	L (N)	3648.85
t (s)	1200.00	THICK	0.009525
		WIDTH	0.0762
k	0.000082		
hA	0.77	12.37202992	1.141188
hA_theory	0.68		
k av	0.0000545		
Tinf pred	33	deg C	
	92	deg F	
% diff	8.87		
diff	3.2528578	°C	

6x2		TEST 1	
Tw(t)	101.00	Tw(t) (C)	38.33
Ti	79.50	Ti (C)	26.39
Tinf	108.00	Tinf (C)	42.22
Tamb	72.50	Tamb (C)	22.50
V	3.00	V (m/s)	1.34
L	625.00	L (N)	2781.14
t (s)	1200.00	THICK	0.009525
		WIDTH	0.0508
k	0.000049	0.89	
hA	0.63	ha_theory/ha	1.010520147
hA_theory	0.63	0.99	
k av	0.0000545		
Tinf pred	45	deg C	
	113	deg F	
% diff	6.20		
diff	2.617553213	°C	

8x3 85A		Test 2	
Tw(t)	82.00	Tw(t) (C)	27.78
Ti	78.00	Ti (C)	25.56
Tinf	88.50	Tinf (C)	31.39
Tamb	74.00	Tamb (C)	23.33
V	3.00	V (m/s)	1.34
L	550.00	L (N)	2447.40
t (s)	1200.00	THICK	0.009525
		WIDTH	0.0762
k	0.000063		
hA	0.57	-18.1522237	0.846366
hA_theory	0.68		
k av	0.0000545		
Tinf pred	29	deg C	
	85	deg F	
% diff	6.81		
diff	2.1370399	°C	

6X2		Test 2	
Tw(t)	116.50	Tw(t) (C)	46.94
Ti	89.00	Ti (C)	31.67
Tinf	126.00	Tinf (C)	52.22
Tamb	72.00	Tamb (C)	22.22
V	4.05	V (m/s)	1.81
L	675.00	L (N)	3003.63
t (s)	1200.00	THICK	0.009525
		WIDTH	0.0508
k	0.000048		
hA	0.61	-4.443180083	0.957458399
hA_theory	0.64		
k av	0.0000545		
Tinf pred	55	deg C	
	131	deg F	
% diff	5.16		
diff	2.696272998	°C	

8x3 85A		Test 3	
Tw(t)	92.50	Tw(t) (C)	33.61
Ti	75.00	Ti (C)	23.89
Tinf	112.00	Tinf (C)	44.44
Tamb	74.00	Tamb (C)	23.33
V	4.15	V (m/s)	1.86
L	1225.00	L (N)	5451.02
t (s)	1200.00	THICK	0.009525
		WIDTH	0.0762
k	0.000055		
hA	0.77	8.361243465	1.091241
hA_theory	0.70		
k av	0.0000545		
Tinf pred	46	deg C	
	115	deg F	
% diff	4.23		
diff	1.8786019	°C	

6X2		TEST 3	
Tw(t)	94.00	Tw(t) (C)	34.44
Ti	79.50	Ti (C)	26.39
Tinf	100.00	Tinf (C)	37.78
Tamb	72.00	Tamb (C)	22.22
V	2.00	V (m/s)	0.89
L	620.00	L (N)	2758.89
t (s)	1200.00	THICK	0.009525
		WIDTH	0.0508
k	0.000051		
hA	0.55	-10.25182676	0.90701445
hA_theory	0.61		
k av	0.0000545		
Tinf pred	37	deg C	
	99	deg F	
% diff	1.17		
diff	0.443022357	°C	

8x3 85A		Test 4	
Tw(t)	87.75	Tw(t) (C)	30.97
Ti	80.50	Ti (C)	26.94
Tinf	98.00	Tinf (C)	36.67
Tamb	73.00	Tamb (C)	22.78
V	3.10	V (m/s)	1.39
L	880.00	L (N)	3915.84
t (s)	1200.00	THICK	0.009525
		WIDTH	0.0762
k	0.000062		
hA	0.64	-6.28318272	0.940883
hA_theory	0.68		
k av	0.0000545		
Tinf pred	34	deg C	
	94	deg F	
% diff	6.77		
diff	2.4823483	°C	

6X2		Test 4	
Tw(t)	98.50	Tw(t) (C)	36.94
Ti	73.50	Ti (C)	23.06
Tinf	107.00	Tinf (C)	41.67
Tamb	72.00	Tamb (C)	22.22
V	5.25	V (m/s)	2.35
L	365.00	L (N)	1624.18
t (s)	1200.00	THICK	0.009525
		WIDTH	0.0508
k	0.000055		
hA	0.62	-5.763381727	0.945506832
hA_theory	0.65		
k av	0.0000545		
Tinf pred	41	deg C	
	105	deg F	
% diff	2.80		
diff	1.16499985	°C	

8x3 85A		Test 5	
Tw(t)	94.00	Tw(t) (C)	34.44
Ti	81.00	Ti (C)	27.22
Tinf	111.00	Tinf (C)	43.89
Tamb	73.00	Tamb (C)	22.78
V	3.00	V (m/s)	1.34
L	1310.00	L (N)	5829.26
t (s)	1200.00	THICK	0.009525
		WIDTH	0.0762
k	0.000061		
hA	0.68	0.239052317	1.002396
hA_theory	0.68		
k av	0.0000545		
Tinf pred	42	deg C	
	107	deg F	
% diff	5.21		
diff	2.2851303	°C	

8x3 85A		Test 6	
Tw(t)	102.50	Tw(t) (C)	39.17
Ti	75.50	Ti (C)	24.17
Tinf	126.50	Tinf (C)	52.50
Tamb	72.00	Tamb (C)	22.22
V	6.20	V (m/s)	2.77
L	1250.00	L (N)	5562.27
t (s)	1200.00	THICK	0.009525
		WIDTH	0.0762
k	0.000060		
hA	0.90	18.13008969	1.22145
hA_theory	0.74		
k av	0.0000545		
Tinf pred	56	deg C	
	132	deg F	
% diff	6.25		
diff	3.281466	°C	

6X3		TEST 1	
Tw(t)	106.00	Tw(t) (C)	41.11
Ti	74.50	Ti (C)	23.61
Tinf	134.00	Tinf (C)	56.67
Tamb	72.00	Tamb (C)	22.22
V	6.20	V (m/s)	2.77
L	875.00	L (N)	3893.59
t (s)	1200.00	THICK	0.009525
		WIDTH	0.0762
k	0.000047		1.16
hA	0.66	A_THEORY/H	0.995531
hA_theory	0.66		1.00
k av	0.0000545		
Tinf pred	62	deg C	
	144	deg F	
% diff	9.35		
diff	5.296461902	°C	

10X3		TEST 1	
Tw(t)	79.00	Tw(t) (C)	26.11
Ti	77.00	Ti (C)	25.00
Tinf	83.00	Tinf (C)	28.33
Tamb	70.00	Tamb (C)	21.11
V	6.30	V (m/s)	2.82
L	525.00	L (N)	2336.15
t (s)	1200.00	THICK	0.009525
		WIDTH	0.0762
k	0.000049		1.11
hA	0.66	A_THEORY/H	0.795023586
hA_theory	0.83		1.26
k av	0.0000545		
Tinf pred	27	deg C	
	81	deg F	
% diff	3.00		
diff	0.851032608	°C	

6X3		TEST 2	
Tw(t)	89.50	Tw(t) (C)	31.94
Ti	76.00	Ti (C)	24.44
Tinf	103.00	Tinf (C)	39.44
Tamb	71.00	Tamb (C)	21.67
V	3.00	V (m/s)	1.34
L	800.00	L (N)	3559.85
t (s)	1200.00	THICK	0.009525
		WIDTH	0.0762
k	0.000052		
hA	0.61	-3.08589734	0.970065
hA_theory	0.63		
k av	0.0000545		
Tinf pred	40	deg C	
	104	deg F	
% diff	0.77		
diff	0.303831647	°C	

10X3		TEST 2	
Tw(t)	79.00	Tw(t) (C)	26.11
Ti	77.00	Ti (C)	25.00
Tinf	82.50	Tinf (C)	28.06
Tamb	72.00	Tamb (C)	22.22
V	3.00	V (m/s)	1.34
L	810.00	L (N)	3604.35
t (s)	1200.00	THICK	0.009525
		WIDTH	0.0762
k	0.000052		
hA	0.73	-8.414503535	0.922385813
hA_theory	0.80		
k av	0.0000545		
Tinf pred	28	deg C	
	82	deg F	
% diff	0.73		
diff	0.203907039	°C	

6X3		TEST 3	
Tw(t)	90.00	Tw(t) (C)	32.22
Ti	75.00	Ti (C)	23.89
Tinf	107.00	Tinf (C)	41.67
Tamb	72.00	Tamb (C)	22.22
V	4.00	V (m/s)	1.79
L	625.00	L (N)	2781.14
t (s)	1200.00	THICK	0.009525
		WIDTH	0.0762
k	0.000054		
hA	0.55	-15.3482838	0.86694
hA_theory	0.64		
k av	0.0000545		
Tinf pred	39	deg C	
	103	deg F	
% diff	5.89		
diff	2.455485968	°C	

10X3		TEST 3	
Tw(t)	84.50	Tw(t) (C)	29.17
Ti	71.00	Ti (C)	21.67
Tinf	98.50	Tinf (C)	36.94
Tamb	71.00	Tamb (C)	21.67
V	4.00	V (m/s)	1.79
L	1825.00	L (N)	8120.91
t (s)	1200.00	THICK	0.009525
		WIDTH	0.0762
k	0.000052		
hA	1.10	16.19028953	1.193179161
hA_theory	0.92		
k av	0.0000545		
Tinf pred	41	deg C	
	106	deg F	
% diff	10.62		
diff	3.922343512	°C	

6X3		TEST 4	
Tw(t)	97.00	Tw(t) (C)	36.11
Ti	75.00	Ti (C)	23.89
Tinf	119.50	Tinf (C)	48.61
Tamb	72.00	Tamb (C)	22.22
V	3.00	V (m/s)	1.34
L	1025.00	L (N)	4561.06
t (s)	1200.00	THICK	0.009525
		WIDTH	0.0762
k	0.000055		
hA	0.60	-4.77483258	0.954428
hA_theory	0.63		
k av	0.0000545		
Tinf pred	47	deg C	
	117	deg F	
% diff	2.52		
diff	1.226670822	°C	

10X3		TEST 4	
Tw(t)	86.00	Tw(t) (C)	30.00
Ti	76.00	Ti (C)	24.44
Tinf	95.50	Tinf (C)	35.28
Tamb	71.00	Tamb (C)	21.67
V	6.30	V (m/s)	2.82
L	1250.00	L (N)	5562.27
t (s)	1200.00	THICK	0.009525
		WIDTH	0.0762
k	0.000052		
hA	1.17	1.254299344	1.012702319
hA_theory	1.15		
k av	0.0000545		
Tinf pred	36	deg C	
	97	deg F	
% diff	2.66		
diff	0.93701678	°C	

6X3		TEST 5	
Tw(t)	94.50	Tw(t) (C)	34.72
Ti	75.00	Ti (C)	23.89
Tinf	112.00	Tinf (C)	44.44
Tamb	73.00	Tamb (C)	22.78
V	5.25	V (m/s)	2.35
L	550.00	L (N)	2447.40
t (s)	1200.00	THICK	0.009525
		WIDTH	0.0762
k	0.000064		
hA	0.66	0.3651374	1.003665
hA_theory	0.65		
k av	0.0000545		
Tinf pred	41	deg C	
	106	deg F	
% diff	7.37		
diff	3.27584722	°C	

10X3		TEST 5	
Tw(t)	81.00	Tw(t) (C)	27.22
Ti	74.50	Ti (C)	23.61
Tinf	90.00	Tinf (C)	32.22
Tamb	74.00	Tamb (C)	23.33
V	3.10	V (m/s)	1.39
L	1050.00	L (N)	4672.31
t (s)	1200.00	THICK	0.009525
		WIDTH	0.0762
k	0.000065		
hA	0.88	8.369520873	1.091339923
hA_theory	0.81		
k av	0.0000545		
Tinf pred	31	deg C	
	89	deg F	
% diff	2.48		
diff	0.800598585	°C	

6X3		TEST 6	
Tw(t)	87.50	Tw(t) (C)	30.83
Ti	72.00	Ti (C)	22.22
Tinf	102.00	Tinf (C)	38.89
Tamb	71.00	Tamb (C)	21.67
V	6.30	V (m/s)	2.82
L	440.00	L (N)	1957.92
t (s)	1200.00	THICK	0.009525
		WIDTH	0.0762
k	0.000056		
hA	0.64	-4.29567265	0.958813
hA_theory	0.66		
k av	0.0000545		
Tinf pred	38	deg C	
	100	deg F	
% diff	2.82		
diff	1.09839247	°C	

Appendix A.2: Calculation of Biot Number

0.35	Rk
1.68	1/hA
0.10	Bi
0.01	Error

Designing with plastics— cast solid-polyurethane industrial tires

Polyether-based liquid urethane systems make better press-on tires and wheels because of lower internal heat buildup, the main cause of blowouts.

By A. I. Hoodbroy, Chemical Division,
Uniroyal, Inc., Naugatuck, Conn.

The use of liquid polyurethane elastomers for the manufacture of solid industrial press-on tires, pallet rollers (load wheels), and caster wheels has increased rapidly during recent years. High load-bearing capacities coupled with excellent abrasion and chunk-out resistance make polyurethanes ideal for use in solid tires and wheels.

Unfortunately, there has been a lack of dynamic engineering data for the various available types and grades of liquid polyurethane elastomers. As a result, urethane tires have been made from several different commercial elastomers with a mixed degree of success in their performance in the overall marketplace.

The major problem has been polymer failure due to internal heat buildup. Lack of dynamic data for polyurethane tires has also prevented forklift-truck manufacturers from designing trucks which could take full advantage of the desirable properties of polyurethane tires. Furthermore, lack of such data has inhibited the development of polyurethane tires having the optimum performance/cost relationship.

A systematic procedure has been developed to select the polyurethane elastomers best suited for specific tire applications. The procedure involves theoretical considerations, along with actual dynamic data generated for several polymers. Using these procedures will help in the selection of polyurethane elastomers for the design of tires which will not fail as a result of internal heat generation, often after limited use.

Defining design parameters

To design a polyurethane tire or wheel it is necessary to know the load to be carried, in many practical situations the tire or wheel size is fixed. In such cases load-bearing data for polyurethane tires/wheels established by the Tire & Rim Association should

be used.

However, the tire size used in the calculations should be based on the finished tire rather than the nominal tire size. For example, a nominal 18 by 5 by 12-1/8 inch tire may have actual dimensions of 17-7/8 by 4-1/4 by 12-1/8 inches. Three specific dimensions must be established, namely the inside and outside radii of the polyurethane tread, and the working width of the tread.

Another parameter that must be determined is the compression modulus (E) which is a function of the hardness of the polyurethane selected. The Table lists E values related to hardness (Shore D) for various commercially available polyurethane elastomers. However, it is imperative that the exact E value be known for the specific elastomer system to be used. Such data can be obtained from the suppliers of liquid polyurethane molding systems.

Compression modulus of
typical polyurethanes as a
function of hardness.

Hardness, Shore D	Compression modulus, psi
40	4,400
45	6,800
50	9,000
55	15,000
60	18,000

Tire calculations

Tire deflection: The deflection for a specific tire size under a known loading can be calculated from the following equation:

$$U = \left[\frac{0.75 W (b - a)}{E S (8b)^{1/2}} \right]^{2/3}$$

Where U is the deflection in inches;

W is the loading in pounds; a is the inside radius of the polyurethane tread in inches; and b the outside radius. E is the compression modulus in psi; and S the actual tire width in inches.

Tire deflection should be calculated for the hardness of the polyurethane tread desired by using the appropriate compression-modulus value. The procedure may have to be repeated using a harder grade polyurethane (larger value for E), if it is determined that the softer grade compound selected initially will exceed safe operating temperatures for the specific load and speed conditions.

Tire footprint: The area of the tire footprint for the specific hardness grade chosen can be calculated from the following equation:

$$P = 2S[b^2 - (b - U)^2]^{1/2}$$

Where P is the area of the footprint in square inches.

Load stress on the tire: Tire stress for the specific grade of urethane chosen can be calculated from the following equation:

$$L = \frac{W}{P}$$

Where L is the load per square inch of footprint expressed in psi.

Optimum dynamic performance

Polyurethanes can be formulated in a multitude of combinations of their basic ingredients. Internal heat buildup is a function of the spine (polyether or polyester) and level of curing agent. Thus, dynamic-heat-buildup data must be available for the commercially available polyurethane resins recommended for use in tires and wheels.

Figure 1 shows heat-buildup data for two polyether- and two polyester-based MOCA-cured polyurethanes, each in two hardness grades, tested